CHALMERS
UNIVERSITY OF TECHNOLOGY

Development of a method for heat shock stress assessment in yeast based on transcription of specific genes

Received: 20 November 2019 | Revised: 22 May 2021 | Accepted: 22 June 2021

DOI: 10.1002/yea.3658

RESEARCH ARTICLE

Yeast WILEY

Development of a method for heat shock stress assessment in yeast based on transcription of specific genes

Eugenio Meza[1] | Ana Joyce Muñoz-Arellano[1] | Magnus Johansson[1] | Xin Chen[1,2] | Dina Petranovic[1]

[1]Division of Systems and Synthetic Biology, Department of Biology and Biological Engineering, Chalmers University of Technology, Gothenburg, Sweden

[2]Novo Nordisk Foundation Center for Biosustainability, Chalmers University of Technology, Gothenburg, Sweden

Correspondence
Xin Chen, Division of Systems and Synthetic Biology, Department of Biology and Biological Engineering, Chalmers University of Technology, Kemivägen 10, Gothenburg, Sweden; Novo Nordisk Foundation Center for Biosustainability, Chalmers University of Technology, Kemivägen 10, Gothenburg, Sweden.
Email: cxin@chalmers.se

Funding information
Novo Nordisk Foundation Center for Biosustainability, Grant/Award Number: 21210022; Chalmers Foundation, Grant/Award Number: C2007/778; Kristina Stenborg Foundation, Grant/Award Number: C2012/1241

Abstract

All living cells, including yeast cells, are challenged by different types of stresses in their environments and must cope with challenges such as heat, chemical stress, or oxidative damage. By reversibly adjusting the physiology while maintaining structural and genetic integrity, cells can achieve a competitive advantage and adapt environmental fluctuations. The yeast *Saccharomyces cerevisiae* has been extensively used as a model for study of stress responses due to the strong conservation of many essential cellular processes between yeast and human cells. We focused here on developing a tool to detect and quantify early responses using specific transcriptional responses. We analyzed the published transcriptional data on *S. cerevisiae* DBY strain responses to 10 different stresses in different time points. The principal component analysis (PCA) and the Pearson analysis were used to assess the stress response genes that are highly expressed in each individual stress condition. Except for these stress response genes, we also identified the reference genes in each stress condition, which would not be induced under stress condition and show stable transcriptional expression over time. We then tested our candidates experimentally in the CEN.PK strain. After data analysis, we identified two stress response genes (*UBI4* and *RRP*) and two reference genes (*MEX67* and *SSY1*) under heat shock (HS) condition. These genes were further verified by real-time PCR at mild (42°C), severe (46°C), to lethal temperature (50°C), respectively.

Take Away

- Bioinformatics pipeline provides a reliable tool to identify stress response and reference genes.
- *UBI4* and *RRP5* are confirmed as heat shock stress response genes.
- *MEX67* and *SSY1* are confirmed as reference genes under heat shock condition.

KEYWORDS
heat shock stress, qPCR, stress assessment, transcriptomics, unfolded protein response, yeast

Ana Joyce Muñoz-Arellano and Magnus Johansson contributed equally to this work and should be considered joint second authors.

1 | INTRODUCTION

The yeast *Saccharomyces cerevisiae* is a unicellular microorganism that has been used by humans for thousands of years, for example, in production of leaven bread and alcoholic beverages. As an eukaryotic organism, *S. cerevisiae* has been extensively used as a model system to study the cellular and molecular biology (Botstein & Fink, 1988, 2011; Petranovic & Nielsen, 2008; Petranovic et al., 2010), and when the yeast genome was sequenced and annotated, it was found that one third of its genome has clear human homologs in the human genome (Botstein et al., 1997; Goffeau et al., 1996). Study has showed that a substantial portion of conserved yeast essential genes can be substituted by their human orthologs, indicating that the similar roles are performed in both organisms (Kachroo et al., 2015). It makes yeast a valuable model for study of fundamental cell biology as well as the etiology and therapeutics of human diseases.

Microorganisms in an ecological niche tend to maximize their growth and their biomass formation; thus, the fastest growing organisms will consume the preferred resources (Reich & Meiske, 1985). When the environmental conditions change, the cells perceive a stress (Gasch, 2007). Different stresses have been studied in yeast, and the regulatory pathways that govern the responses have been largely elucidated. It has been reported that a general stress response is induced regardless of the types of stress exerted on cells, and due to this, when the yeast cells are exposed to a mild stress, they are facilitating stress responses and capable of re-establishing cellular homeostasis. When the buffering capacity proves inadequate to restore cellular homeostasis, the apoptosis program will be switched on to remove irreversible damaged cells (Gasch, 2007; Szegezdi et al., 2006; Verghese et al., 2012). Specific stress responses occur in different cellular compartments, for example, the heat shock (HS) (Martelli et al.) stress in the cytosol, the reactive oxygen species (ROS) stress in the mitochondria, and the unfolded protein stress (UPR) in the endoplasmic reticulum (ER) (Fannjiang et al., 2004; Longo et al., 1997; Madeo et al., 1997; Martelli et al., 2001). Prolonged and severe stresses can damage DNA, proteins, and membrane lipids, which in turn can trigger programmed cell death (Hauptmann & Lehle, 2008; Madeo et al., 2002; Uren et al., 2000; Yang et al., 2008). The assessment of stress processes can be done by measuring the cell viability, which reflects the ability of cell division and cell proliferation, and the cell vitality, which is defined as the physiological capabilities and metabolic activity of cell (Carmona-Gutierrez et al., 2018). Nevertheless, an impaired cell proliferation or metabolic activity does not necessarily lead to cell death; combination of multiple techniques can be helpful to determine cell death, such as propidium iodide (PI) staining (Mirisola et al., 2014), clonogenicity assay (Carmona-Gutierrez et al., 2010), growth rate measurement (Jung et al., 2015), and assessment of specific enzymes (Kwolek-Mirek & Zadrag-Tecza, 2014). Additionally, use of fluorescent dyes and/or fluorescent proteins to monitor specific compartments is highly informative (Munoz et al., 2012; Wloch-Salamon & Bem, 2013). However, sensitive markers to detect early stress induction and potentially predict the fate of the culture could save millions of USD in fermentation-based bioproduction costs. Being able to monitor the culture very early in the process in a cheap, easy, quick, and reliable way is still a grand challenge of the fermentation industry.

In this paper, we propose the use of transcriptional responses as an early marker for different cell stresses, especially focusing on HS response. Gasch et al. (2000) studied the transcriptional response of yeast *S. cerevisiae* subjected to 10 different stress conditions over time, which are the HS, the stationary phase (ST phase), the nitrogen depletion (N deplt), the hydrogen peroxide (H_2O_2), the dithiothreitol (DTT) stress, the amino acids starvation (AA stv), the diamide, the hyperosmotic (HYPER-OS), the hypoosmotic stress (HYPO-OS), and menadione-induced oxidative stress. Using these data, we developed the bioinformatics tool to select stress response genes under specific stress conditions, based on the correlation and the covariance by the Pearson analysis and the principal component analysis (PCA) (Mansson et al., 2004; Yeung & Ruzzo, 2001). The selection of stress response genes was based on their specificity, that is, how unique is the transcriptional response, in a given stress, when compared with other stresses. We also selected the reference genes in each stress condition, which would not be induced under stress condition and show no transcriptional change over time. HS is the most fundamental stress that yeast cells experience, which includes many conserved features viewed as central to our understanding of eukaryal cell biology (Morano et al., 2012). The optimal growth temperature for *S. cerevisiae* is between 25°C and 30°C. At temperature higher than 37°C, yeast cells activate a conserved transcriptional response termed the heat shock response (HSR) and alter other physiological components (Verghese et al., 2012). Many transcription factors activate the transcription of cytoprotective genes leading to metabolic reprogramming, which is essential for the thermotolerance under acute and lethal temperatures (Mühlhofer et al., 2019; Sanchez & Lindquist, 1990). In this study, we identified two HS stress response genes (*UBI4* and *RRP5*) and two HS reference genes (*MEX67* and *SSY1*) from the transcriptional data analysis. They were further verified by qPCR under HS stress. The HS stress was induced at three different levels: mild (42°C, the cells are capable to cope with), severe (46°C, measured as decrease in cellular viability and vitality), and lethal (50°C). The cell viability and vitality were measured by the specific growth rate, spot dilution assay, and FUN1 staining, respectively. Yeast cell death is often accompanied by oxidative damage, and production of ROS is one of the major secondary consequences involved in HS stress. The mitochondrial damage (MitoTracker staining) and ROS production (DHR123 staining) were evaluated as well after HS stress.

2 | MATERIALS AND METHODS

2.1 | Data

The transcription data were kindly provided by Prof. Patrick O. Brown (Gasch et al., 2000). This data set comprises the transcriptional response of *S. cerevisiae* to 10 stresses at different time points, where

the transcriptional response is regarded as the fold change between the ratio of Cy5/Cy3 fluorescence in the stress condition versus the control (Gasch et al., 2000).

2.2 | Statistical analysis of the stress transcription response

For each stress, the time point with the highest number of upregulated genes was selected and included into a matrix; therefore, a 10×6152 matrix was generated. These data were used to perform statistical analysis to assess the likeliness of identifying specific upregulated genes in each stress condition (Figure 1). The Pearson analysis was performed to assess the correlation between different stresses (Mansson et al., 2004). This was done by comparing the selected time point of the stress_i with the selected time points of the remaining nine stresses, the selected time point of the stress_j with the selected time points of remaining nine stresses, and so on. The R^2 coefficients, which represent the probability that two data sets are related (−1, 0, 1 for inversely correlated, noncorrelated, and correlated, respectively), were clustered in a heat map by Cluster 3.0 software (J. Nolan et al., 2004). The covariance analysis was performed to the 10×6152 matrix by PCA (Yeung & Ruzzo, 2001). The data were analyzed in R with prcomp (Development Core Team, 2011) and visualized with pca2d package (Weiner, 2013).

2.3 | Selection of stress response genes

The quality of the raw data in the stress_i was enhanced by discarding the genes that presented more than 20% of missing data (J. Nolan et al., 2004; Ouyang et al., 2004) and/or with unknown functions (Figure 2). The genes with at least one time point with a fold change ≥ 2 and with a difference between the highest and lowest fold change values ≥ 2 were selected. The resulting gene sets of the 10 stresses were compared between each other to search for common genes that were induced in all tested stress, but not in standard conditions, as well as stress response genes that were highly expressed in a given stress, but not in others. Two stress response genes were selected from each data set for specific stress induction, and these two genes (response genes for a specific stress) were found not to be highly induced in any other stress conditions (Figure 2). The stress response genes were also selected to be transcriptionally nonrelated; that is, they are categorized in different gene ontology terms (GO annotation) (Cherry et al., 1997).

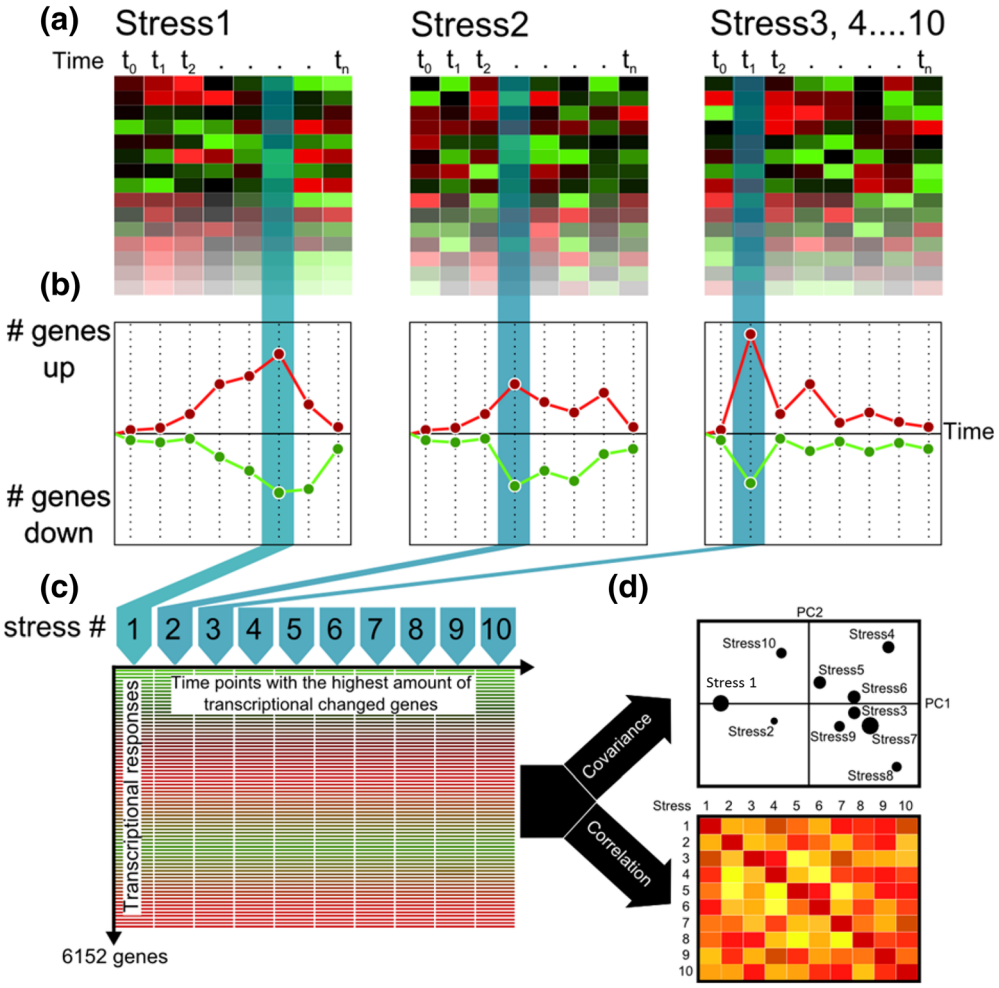

FIGURE 1 The statistical analysis of the stress transcriptional response. Pipeline to analyze the likeliness of finding specific markers for the 10 different stresses. (a) After the stress_i (10 different stresses) was exerted, the transcriptional response was followed during different time points ($t_0 \ldots t_n$). (b) In each time point, the number of upregulated genes was determined and the time point with the highest number of upregulated genes was selected. (c) After doing this selection to the 10 stresses, a 10×6152 matrix was generated. (d) In order to assess if the stress responses shared some degree of correlation, a Pearson analysis was performed and the R^2 coefficient was plotted as a heat map. To determine the amount of change in each stress, the transcriptional responses in the 10×6152 matrix were analyzed by a principal component analysis (PCA) and plotted in a PCA plot [Colour figure can be viewed at wileyonlinelibrary.com]

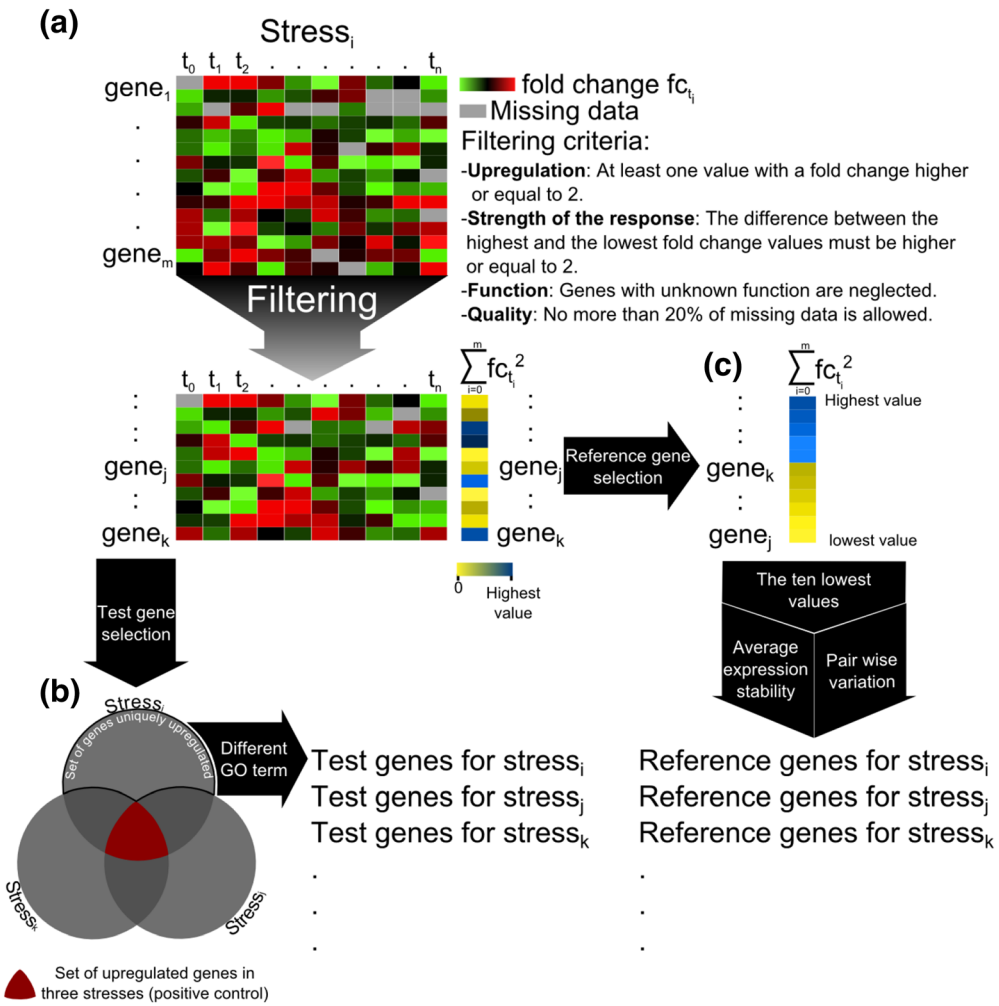

FIGURE 2 Pipeline for the selection of the test and the reference genes. (a) Each data set (stress$_i$) of the 10 stresses was filtered following the criteria depicted here; this generates a new data set with a lower number of genes. (b) For the test gene selection, the data set obtained after filtering (stress$_i$) was compared with the other filtered data sets (stress$_j$, stress$_k$, …) and the genes upregulated specifically for each stress and the genes upregulated in all the stresses were identified as test genes and as positive control genes, respectively. (c) To select the reference genes, for each gene in the data set, the sum of the square of the fold changes in the time points was calculated (Σ_i fc$_i^2$). These values were arranged from the highest to the lowest values. The statistical analysis method was performed to the 10 lowest values, and the *ACT1* transcriptional values were added as comparative reference. These procedures delivered two stress response genes and two reference genes per stress condition [Colour figure can be viewed at wileyonlinelibrary.com]

2.4 | Selection of reference genes

The 10 genes with the lowest Σ_i fc$_i^2$ value were selected and arranged from the lowest to the highest value, where the fc$_i$ is the fold change value of the gene *x* in the "i" time (Figure 2). The statistical method developed by Vandesompele et al. (2002) was used to select the two best reference genes, that is, the genes that would not be induced in any stress condition and show no transcriptional change over time (Figures S1 and S2). This algorithm performs a pairwise variation analysis that sets the minimal number of reference genes that are necessary for an adequate normalization of the qPCR data. The pairwise variation is a measurement of the standard deviation of the normalization factor resulting from each iteration round of the reference gene data set (RGDS). This value was set to 0.15 as a cut-off to describe that the addition of an extra reference gene has no significant effect in the normalization of qPCR data, setting the minimal amount of reference genes for normalization. The gene coding for actin (*ACT1*) was used as a comparative reference gene (Aad et al., 2010; Teste et al., 2009; Vandesompele et al., 2002).

2.5 | Strains and media

The strain used for this work was *S. cerevisiae* CEN.PK 113-11C (*MAT***a** *his3Δ1 ura 3-52 MAL2-8c SUC2*) (Entian & Kötter, 1998). Cells were cultivated in shake flasks, in YPD medium containing 10 g L^{-1} yeast extract, 20 g L^{-1} peptone from casein, and 20 g L^{-1} glucose, at 30°C and at 200 rpm.

2.6 | Growth, induction of stress, and sampling

An overnight culture was used to inoculate 100 ml of medium, at $OD_{600} = 0.1$. When OD_{600} reached 0.4, cells were exposed to different levels of stress and samples for RNA extraction were taken after 60 min. Specific growth rate was determined by measuring OD_{600} every 90 min. The HS stress was performed at temperatures 42°C, 46°C, and 50°C, respectively, and the DTT stress was induced with 2.5, 5.0, and 7.5 mM of DTT, respectively (Sigma-Aldrich).

2.7 | RNA extraction and qPCR

2×10^7 cells were harvested by centrifugation at 12,000× g for the RNA extraction using the RNeasy® kit from QIAGEN following the manufacturer's protocol. The DNase treatment was performed to remove the genomic DNA (Bustin et al., 2009; T. Nolan et al., 2006; Udvardi et al., 2008). The RNA concentration and quality assessment were done by nanodrop 2000 spectrophotometer determining the absorbance at 260 nm (nucleic acids), 280 nm (protein), and 230 nm (other contaminants) (Becker et al., 2010). One percent of agarose gel was used to visualize the 28S, 18S, and 5S ribosomal RNA bands as a method to assess RNA quality. The RNA concentration was set to 500 ng/μl with RNase-free water, and 10 μl were used for first-strand cDNA synthesis using the QuantiTect Reverse Transcription kit from QIAGEN following the manufacturer's recommendations. Primers for the test genes were designed in the primer3 software (Rozen & Skaletsky, 2000) and synthesized by Sigma-Aldrich. The validation of the primers was done with serial 10-fold dilutions of cDNA, and then the qPCR was performed including a melting curve test. The primer dimers existence and the efficiency of qPCR reaction were determined (Ruijter et al., 2009; Schefe et al., 2006). A list of primers used in this work is shown in Table S1. The qPCR reactions were done in Mx3005P Agilent technologies equipment using the Brilliant III Ultra-Fast SYBR® Green qPCR mix, following the manufacturer's recommendations. The threshold and the base line were set, and the C_t was obtained using the MxPro software (Agilent). *ACT1* was used as a reference gene to normalize RNA levels. The C_t values were used to determine the transcriptional fold changes with the ΔC_t method (Schefe et al., 2006), using as efficiency value obtained from the primer validation.

2.8 | Assessing the phenotypes of stress

After 4 h of stress induction, 1 ml of cell culture was set at $OD_{600} = 0.2$ (4×10^6 cells) and diluted in 10-fold series (10^{-1}, 10^{-2}, 10^{-3}). A total of 3.5 μl of each suspension was spotted on YPD plate. The plate was incubated at 30°C for 2–3 days.

For the same culture, 2×10^7 cells were harvested by centrifugation at 12,000× g. The cell pellets were resuspended and used for staining with FUN1 [2-chloro-4-(2,3-dihydro-3-methyl-(benzo-1,3-thiazol-2-yl)-methylidene)-1-phenylquinolinium iodide] (Thermo Fisher Scientific), MitoTracker green FM (Thermo Fisher Scientific), and dihydrorhodamine 123 (DHR123, Sigma-Aldrich) dyes for assessing the metabolic activity, mitochondrial damage, and ROS production, respectively (Chen et al., 2017; Munoz-Arellano et al., 2018; Qin et al., 2008).

Images from stained cells were taken on an inverted Leica AF 6000 fluorescence microscope with an HCX PL APO CS 100.0 × 1.40 OIL objective, captured with a DFC 360 FX camera and the Leica Application Suite software. The quantification of cells involved the analysis of at least 300 cells per sample from three independent experiments. The brightness and the gain settings were adjusted to avoid the background noise and to discard false positives during the counting.

For the FUN1 staining (Munoz-Arellano et al., 2018), the cell pellet was washed with 1 ml of HEPES buffer (10-mM HEPES, 2% glucose, pH 7.2) and centrifuged at 12,000× g. The cell pellet was resuspended in 250 μl of HEPES buffer containing the FUN1 dye at a final concentration of 15 μM. The cell suspension was incubated at room temperature in the dark for 30 min. After the incubation, cells were centrifuged at 12,000× g, and 2 μl of the cell pellet were loaded on a microscope slide for inspection by fluorescence microscopy using the DIC and FLUO-RFP filters. Metabolically active cells can process the dye in the vacuole where it forms compact structures with striking red fluorescence. Metabolically nonactive cells give out a uniform glow with no discernable red structures.

For the determination of mitochondrial, the cell pellet was suspended in 1 ml of HEPES buffer (10-mM HEPES, 5% glucose, pH 7.4) containing the 100-nM MitoTracker green FM dye (Keij et al., 2000). The cell suspension was incubated at room temperature in the dark for 15 min. After the incubation, the cells were centrifuged at 12,000× g, and 2 μl of the cell pellet were loaded on a microscope slide for inspection by fluorescence microscopy using the DIC and FLUO-GFP filters.

The production of ROS was determined by staining the cells with DHR123 (Qin et al., 2008). The cell pellet was washed three times with water and resuspended in 1 ml of sodium citrate buffer (50-mM sodium citrate, 2% glucose, pH 5.0) containing 50-μM DHR123. The cell suspension was incubated at room temperature in the dark for 15 min. After the incubation, the cells were centrifuged at 12,000× g, and 2 μl of the cell pellet were loaded on a microscope slide for inspection by fluorescence microscopy using the DIC and FLUO-YFP filters. Cells showing an intense fluorescence were treated as ROS accumulating cells.

2.9 | Statistical analyses

All experiments were performed in biological triplicates, unless specified explicitly. Significance of differences between results was determined using two-tailed, Student's *t* tests. Data were presented as the mean ± SD. A p-value < 0.05 was considered statistically significant, unless specified explicitly.

3 | RESULTS

We used genome wide transcription data (Gasch et al., 2000), which comprise the transcriptional responses of 6152 genes during different time points, under 10 different stresses. For each stress, the time point with the highest number of upregulated genes was selected and included in a final 10 × 6152 matrix (Figure 1). Each time point was compared with the remaining 9 time points to determine correlation by the Pearson analysis, whereas the 10 × 6152 matrix was analyzed by PCA to assess the covariance of the stresses (Figure 1) (Mansson et al., 2004; Yeung & Ruzzo, 2001).

3.1 | Correlation analysis

The correlation analysis allows determination of the degree of association between two variable changes; this degree of association is represented by the R^2 coefficient. The R^2 coefficients, resulting from the comparisons of the transcriptional responses at the time points with the highest number of upregulated genes per stress (10 stresses in total), were arranged in a 10 × 10 matrix and examined by cluster analysis (Figure 3a). Four clusters were analyzed considering the average degree of correlation within stresses; this decreases from A_1 towards A_4 (Figure 3a), where in A_1, the HS and the H_2O_2 stresses had a high correlation with the diamide stress (68% and 48%, respectively) also, in a lower degree, between them (41%). The HS stress displayed some degree of correlation with the stresses grouped in the cluster A_2: 31% for the DTT stress, 46% for the hyperosmotic stress, and 41% for the amino acid starvation stress. This analysis suggests that the HS stress activates a global response that shares features (with respect to the number of significantly changed genes) with the stresses within the A_1 and A_2 clusters (47% of average correlation). Moreover, the average correlation that the DTT, the H_2O_2, the diamide, the hyperosmotic, and the amino acid starvation stresses had between them was 32%. This implies that the transcriptional responses to these stress conditions are more similar to the HS response (with respect to the number of significantly changed genes) than with each other. The third cluster, A_3, comprises the amino acid starvation, the nitrogen depletion, and the transition to stationary phase. The amino acid starvation stress presented 35% of average correlation with the stresses of the cluster A_2 and 25% of correlation with the stresses of the cluster A_3. Conversely, the average correlations that the nitrogen depletion and the stationary phase stresses had with the A_2 stresses were 13% and 16%, respectively, which were lower than the average value of 25% observed from the A_3 cluster. It is worth noting that most of the upregulated genes were found in the stationary phase, the nitrogen depletion, and the HS stresses (Table S2), even though there was low correlation among them (25% of correlation between the stationary phase and nitrogen depletion, 24% between the stationary phase and HS, and 16% between nitrogen depletion and HS). The A_4 cluster comprises the stress induced with menadione and the hypoosmotic treatment having the lowest correlation values. Interestingly, even though menadione is known to induce the generation of ROS (Kim et al., 2011), the transcriptional response under the menadione treatment and the H_2O_2 had only a 31% of correlation, whereas the average correlation with the other stresses was 9%. The lowest average correlation was between the hypoosmotic stress and any other

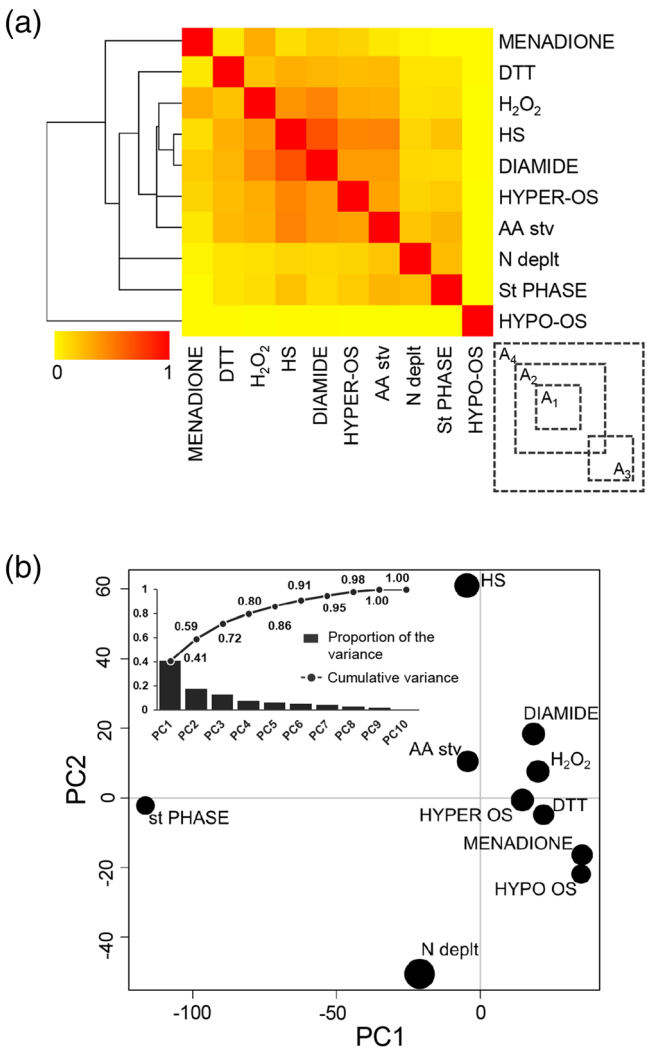

FIGURE 3 Transcriptional data analysis. (a) Pearson correlation analysis of the degree of correlation between the 10 studied stresses based on number of transcriptionally changed genes. The red color represents a correlation value of 1 (100% of probability that the changes between the two stresses are associated), whereas the yellow color represents a correlation value of 0 (0% of probability that the changes between the two stresses are associated). A representation of the analyzed areas (A_1–A_4) is marked in dotted squares. (b) The principal component analysis (PCA) of all the stress conditions. This analysis is performed to the transcriptional response of the time point with the highest number of upregulated genes in the data from Gasch et al. per stress (Section 2 and Figure 1). The two-dimensional graph is based on the PCAs with the two highest values of variance (PC1 and PC2). The proportion and the cumulative variance are depicted in the bar graph in the upper left corner of the figure [Colour figure can be viewed at wileyonlinelibrary.com]

stress response (0.6%), but none of the correlations were negative meaning that the stress responses were not exclusive (Figure 3a).

3.2 | Covariance analysis

The PCA gives the information about similarity of the changes that a group of variables have, by measuring their variance (Yeung & Ruzzo, 2001). The position of each stress in the plot gives information about how unique their variance is, therefore making it possible to assess the likeness to find specific upregulated genes in the stress conditions. Figure 3b showed the amount of variance through the 10 dimensions of the data set. The first and second PCA components clearly separated 10 different stresses, which accounted for 41% and 18% of variance, respectively. Accordingly, as previously discussed, in the stationary phase, the nitrogen depletion, and the HS stresses, it was feasible to find upregulated specific genes because the change in their variance was unique as they separated from the other stresses in the PCA plot (Figure 3b). In addition, the overall changes of the transcriptome during the diamide, H_2O_2, AA starvation, hyperosmotic and hypoosmotic, DTT, and menadione stresses were similar (Figure 3b).

3.3 | Selection of stress response genes

To further select the stress response genes, the data set was filtered, and the quality of the data was assessed as described in Section 2. The genes with at least one time point with a fold change ≥ 2 and with a difference between the highest and lowest fold changes ≥ 2 were selected (Figures 2 and S1). The aim of the filtering process was to enrich the data set with highly upregulated genes. The number of upregulated genes varied with the type of stress evaluated, and in the stationary phase, 48% of the genes were upregulated whereas in the hypoosmotic stress, only 1.7% of the genes were upregulated (Figure S1). In the HS, the H_2O_2, and the DTT stresses, the number of upregulated genes was 310, 90, and 50, respectively (Table S2).

Thus, after the filtering process, the genes that were upregulated only in a specific stress condition were considered as potential markers for the stress. In the stationary phase stress, the highest number of uniquely upregulated genes represented 3.5% of the open reading frames in the array (6152 genes), whereas the uniquely upregulated genes for the diamide and the hyperosmotic stresses only represented 0.065% of the open reading frames in the array (Table S2). In addition to the filtering process, two criteria were used to choose stress response genes: high expression values in a given stress condition, but not in others and transcriptionally nonrelated, which means they are categorized within different GO terms. GO terms are defined by the *S. cerevisiae* genome database (SGD) (https://www.yeastgenome.org/) (Cherry et al., 1997; Cherry et al., 2012). Two uniquely upregulated genes were selected from each stress condition (Table 1). For the HS stress, *RRP5* and *UBI4* were selected as the stress response genes. The transcriptional responses for *RRP5* and *UBI4*, indicating the difference between the highest and lowest transcriptional values, were 8.8 and 8.3, respectively. *RRP5* and *UBI4* are within different GO terms, the former as "associated with rRNA processing" and the latter as "involved in protein catabolic process." These two genes were chosen for the qPCR evaluation under the HS stress. To verify if they were specifically upregulated for the HS stress, their mRNA levels were also tested under DTT stress condition. The genes *KAR2* and *ERO1*, which were previously reported to be induced under both HS stress and DTT stress conditions (Kimata et al., 2006; Kohno et al., 1993), were included as positive controls to ensure that we have indeed induced the stresses. The list of proposed stress response genes is shown in Table 1.

3.4 | Selection of reference genes

The selection of a reference gene is crucial for the analysis of the transcriptional response by qPCR, and one standard reference gene for all the possible conditions is not an optimal strategy (Aad et al., 2010; Teste et al., 2009; Vandesompele et al., 2002). The reference genes should not be induced under the given stress condition and have a stable transcriptional expression over time. These genes were selected from the genome wide transcriptional response (Gasch et al., 2000). The genes with the smallest transcriptional changes over different time points (RGDS) for each stress were selected, the sum of squares for each transcriptional value in each stress condition ($\Sigma_i fc_{ti}^2$) as indicated in Figure S1. The transcriptional stability of each gene in the RGDS in the different stress conditions was assessed by the geometric average analysis with the GEnorm algorithm (Vandesompele et al., 2002), which measures the dispersion of the RGDS. The algorithm subtracts the transcriptional data of the gene with the highest expression stability value and in an iterative calculation process. In this analysis, the *ACT1* gene transcriptional profiles were included as a control because this gene is often used as a reference gene for qPCR experiments (Figure S2). The contribution of this gene to the average expression stability is more significant in the stationary phase, the nitrogen depletion, the DTT, the hyperosmotic, and the menadione stresses. This is supported after a Pearson analysis performed to the average stability statistics of each stress with and without the *ACT1* gene as reference (Table 2).

According to the analysis, no more than two reference genes in each stress condition were selected because all the standard deviations for the normalization factors were below the cut-off (Figure S2). For the HS stress, *MEX67* and *SSY1* were selected as the reference genes. *MEX67* encodes a poly(A) RNA binding protein, which is involved in nuclear mRNA export from nucleus. *SSY1* belongs to the amino acid sensor system and is responsible for regulation of amino acid transport. The proposed reference genes are listed in Table 2.

3.5 | Induction of HS stress

Cells were grown to middle exponential phase and exposed for 60 min to different levels of HS stress at 42°C, 46°C, and 50°C,

TABLE 1 List of the HS stress response genes obtained after the filtering process performed on data[a]

Stress	Test genes	GO (process)	Transcriptional response
Heat shock (HS)	*RRP5*	rRNA processing (GO:0006364), ribosome assembly (GO:0042255), ribosomal small subunit biogenesis (GO:0042274), ribosomal large subunit biogenesis (GO:0042273).	8.8
	UBI4	Proteolysis involved in cellular protein catabolic process (GO:0051603), protein modification by small protein conjugation or removal (GO:0070647).	8.3
Stationary phase (st PHASE)	*RPS20*	Cytoplasmic translation (GO:0002181), rRNA processing (GO:0006364), ribosomal small subunit biogenesis (GO:0042274).	8.9
	CKB2	Regulation of protein modification process (GO:0031399), protein phosphorylation (GO:0006468), transcription by RNA polymerase I (GO:0006360), response to chemical (GO:0042221), cellular response to DNA damage stimulus (GO:0006974), transcription by RNA polymerase III (GO:0006383), peptidyl-amino acid modification (GO:0018193).	7.8
Nitrogen depletion	*LEU1*	Cellular amino acid metabolic process (GO:0006520).	4.8
(N deplt)	*APT2*	Nucleobase-containing small molecule metabolic process (GO:0055086).	3.8
Hydrogen peroxide (H_2O_2)	*MOT3*	Response to osmotic stress (GO:0006970), response to chemical (GO:0042221), lipid metabolic process (GO:0006629), transcription by RNA polymerase II (GO:0006366).	6.8
	PPH22	Cytoskeleton organization (GO:0007010), regulation of translation (GO:0006417), cell budding (GO:0007114), organelle assembly (GO:0070925), mitotic cell cycle (GO:0000278), protein dephosphorylation (GO:0006470), vacuole organization (GO:0007033), regulation of organelle organization (GO:0033043).	6.6
Dithiothreitol (DTT)	*BFR2*	Ribosomal small subunit biogenesis (GO:0042274), rRNA processing (GO:0006364).	4
	AXL1	Cell budding (GO:0007114), cytokinesis (GO:0000910), protein maturation (GO:0051604), conjugation (GO:0000746), mitotic cell cycle (GO:0000278).	3.78
Amino acids starvation (AA stv)	*SPO22*	Meiotic cell cycle (GO:0051321), regulation of organelle organization (GO:0033043), regulation of cell cycle (GO:0051726), regulation of protein modification process (GO:0031399), organelle fission (GO:0048285), chromosome segregation (GO:0007059), protein modification by small protein conjugation or removal (GO:0070647), sporulation (GO:0043934), peptidyl-amino acid modification (GO:0018193).	3.4
	IMP1	Protein maturation (GO:0051604), mitochondrion organization (GO:0007005), protein targeting (GO:0006605).	3.1
Diamide	*SPO13*	Organelle fission (GO:0048285), chromosome segregation (GO:0007059), regulation of organelle organization (GO:0033043), sporulation (GO:0043934), meiotic cell cycle (GO:0051321), regulation of cell cycle (GO:0051726).	3.2

TABLE 1 (Continued)

Stress	Test genes	GO (process)	Transcriptional response
	SMP1	Response to osmotic stress (GO:0006970), transcription by RNA polymerase II (GO:0006366), response to chemical (GO:0042221).	2.7
Hyperosmotic (HYPER-OS)	*SAC3*	RNA catabolic process (GO:0006401), nucleobase-containing compound transport (GO:0015931), ribosomal small subunit biogenesis (GO:0042274), mRNA processing (GO:0006397), DNA repair (GO:0006281), mitotic cell cycle (GO:0000278).	3.4
	NDT80	Transcription by RNA polymerase II (GO:0006366), meiotic cell cycle (GO:0051321).	2.4
Menadione	—		
Hypoosmotic (HYPO-OS)	*SCC2*	Chromatin organization (GO:0006325), mitotic cell cycle (GO:0000278), transcription by RNA polymerase II (GO:0006366), regulation of cell cycle (GO:0051726), chromosome segregation (GO:0007059), organelle fission (GO:0048285), DNA recombination (GO:0006310), regulation of organelle organization (GO:0033043), DNA repair (GO:0006281).	6.7
	COQ1	Lipid metabolic process (GO:0006629), cofactor metabolic process (GO:0051186).	5.6

Note: The genes from different gene ontology (GO) are selected. The transcriptional response column indicates the difference between the highest and lowest transcriptional values from data[a].
[a]Data from Gasch et al.

respectively. Cellular growth, metabolic activity, and viability were determined after the induction of the stress evaluated. For the HS stress at 42°C, a 60% reduction in the specific growth rate was observed compared with control strain growing at 30°C (from 0.48 to 0.28 h^{-1}, $p < 0.05$), whereas cells did not grow at 46°C and 50°C. The metabolic activity was measured with FUN1 staining. This dye passively diffuses into the cell where it is actively transported into the vacuole, forming red rods called cylindrical intravacuolar structures (CIVS). Because the import of the dye into the vacuole is driven by ATP, the formation of CIVS is an indication of metabolic activity. For HS treatment at 42°C, the percentage of cells to form the CIVS structures was similar to control strain, whereas there was a significant reduction in the percent of cells with CIVS structures at 46°C and 50°C. The fractions of metabolically active cells were 12.1% and 4.3% at 46°C and 50°C, respectively, comparing with 91.7% in the control strain ($p < 0.05$; Figure 4a). With the aim of determining whether the reduction of specific growth rate and the metabolic activity were indications of loss of viability, a viability spot test was performed. For the HS treatment at 42°C, no change in viability was observed comparing with control strain at 30°C. Nevertheless, there was a significant reduction in viability when cells were stressed at 46°C, comparing with 30°C. No viable cells were observed at 50°C (Figure 4b).

Mitochondria are pivotal to the survival of cells due to their role as power plants that provide a highly efficient pathway to produce ATP (Andréasson et al., 2019). The mitochondrial network was stained by the MitoTracker Green FM dye. This dye diffuses across the mitochondrial membrane and interacts with the thiol groups of the mitochondrial proteins. The dye accumulates in cells undergoing stress displaying an intense green color with no observation of the mitochondrial network. During the HS stress at 42°C, the mitochondrial network was damaged in 13% of the cell population, whereas during the HS treatment at 46°C and 50°C, more than 50% of the cell population showed mitochondrial damage (Figure 4c). It has been previously established that the mitochondrial damage can lead to excess ROS production (Herrero et al., 2008; Livnat-Levanon et al., 2014). With the aim to determine whether the HS stress conditions that is being tested produce ROS, the cells were stained with DHR123. This dye diffuses across the cell membrane into the cell where it is oxidized by a broad range of ROS to produce rhodamine 123 (emission at 536 nm) and the percent of cells in a population that stained positive for ROS can be quantified. Under HS stress at 46°C and 50°C, the ROS-positive fractions were significantly increased ($p < 0.05$). There were 60% and 59% of cells with ROS-positive staining, respectively, compared with 2.4% in the control strain at 30°C (Figure 4d). The cell population accumulating ROS was in accordance with the cell population with mitochondrial damage (Figure 4c).

3.6 | Assessment of HS stress response by RT-qPCR

The transcriptional response of the HS stress was assessed by qPCR in two conditions, at 42°C and 46°C, after 60 min of induction. The

TABLE 2 List of the reference genes obtained after the statistical analysis with the GEnorm algorithm from data[a]

Stress	Reference genes	GO (process)	Squared Pearson analysis of RGDS	
			Complete	-ACT1
Heat shock (HS)	*MEX67*	Transmembrane transport (GO:0055085), ribosomal subunit export from nucleus (GO:0000054), nucleobase-containing compound transport (GO:0015931).	0.994	0.992
	SSY1	Amino acid transport (GO:0006865), transmembrane transport (GO:0055085), response to chemical (GO:0042221).		
Nitrogen depletion (N deplt)	*NUP42*	Nucleobase-containing compound transport (GO:0015931), response to osmotic stress (GO:0006970), response to chemical (GO:0042221), response to heat (GO:0009408).	0.942	0.996
	REG1	Protein dephosphorylation (GO:0006470), chromatin organization (GO:0006325), transcription by RNA polymerase II (GO:0006366), regulation of protein modification process (GO:0031399), response to starvation (GO:0042594), response to chemical (GO:0042221).		
Hydrogen peroxide (H_2O_2)	*ARG2*	Cellular amino acid metabolic process (GO:0006520).	0.909	0.877
	PFK1	Nucleobase-containing small molecule metabolic process (GO:0055086), carbohydrate metabolic process (GO:0005975), cellular ion homeostasis (GO:0006873), monocarboxylic acid metabolic process (GO:0032787), generation of precursor metabolites and energy (GO:0006091).		
Dithiothreitol (DTT)	*MUD13*	RNA splicing (GO:0008380), nucleobase-containing compound transport (GO:0015931), mRNA processing (GO:0006397), RNA catabolic process (GO:0006401).	0.941	0.991
	SEN15	tRNA processing (GO:0008033), RNA splicing (GO:0008380).		
Amino acids starvation (AA stv)	*CDC15*	Meiotic cell cycle (GO:0051321), organelle fission (GO:0048285), regulation of cell cycle (GO:0051726), cytokinesis (GO:0000910), regulation of organelle organization (GO:0033043), regulation of protein modification process (GO:0031399), mitotic cell cycle (GO:0000278), peptidyl-amino acid modification (GO:0018193), protein phosphorylation (GO:0006468), cytoskeleton organization (GO:0007010).	0.985	0.985
	TIP20	Golgi vesicle transport (GO:0048193), regulation of transport (GO:0051049), cellular response to DNA damage stimulus (GO:0006974), mitotic cell cycle (GO:0000278), regulation of cell cycle (GO:0051726).		
Diamide	*RPD3*	Regulation of cell cycle (GO:0051726), DNA-templated transcription, elongation (GO:0006354), transcription by RNA polymerase I (GO:0006360), chromatin organization (GO:0006325), DNA replication (GO:0006260), regulation of DNA metabolic process (GO:0051052), nucleus organization (GO:0006997), regulation of organelle organization (GO:0033043), transcription by RNA polymerase II (GO:0006366), mitotic cell cycle (GO:0000278), histone modification (GO:0016570), organelle fission (GO:0048285), meiotic cell cycle (GO:0051321), DNA recombination (GO:0006310).	0.934	0.917
	SYS1	Golgi vesicle transport (GO:0048193).		
Hyperosmotic (HYPER-OS)	*SIR4*	DNA repair (GO:0006281), regulation of organelle organization (GO:0033043), chromatin organization (GO:0006325).	0.880	0.972
	SRO77	Exocytosis (GO:0006887), regulation of transport (GO:0051049), Golgi vesicle transport (GO:0048193).		

TABLE 2 (Continued)

Stress	Reference genes	GO (process)	Squared Pearson analysis of RGDS	
			Complete	-ACT1
Menadione	*SRP1*	Protein targeting (GO:0006605).	0.941	0.955
	STU1	Chromosome segregation (GO:0007059), cytoskeleton organization (GO:0007010), organelle assembly (GO:0070925), organelle fission (GO:0048285), mitotic cell cycle (GO:0000278).		
Hypoosmotic (HYPO-OS)	*BOS1*	Golgi vesicle transport (GO:0048193), membrane fusion (GO:0061025), protein targeting (GO:0006605), vesicle organization (GO:0016050), endosomal transport (GO:0016197), organelle fusion (GO:0048284).	0.956	0.940
	TOA1	Transcription by RNA polymerase II (GO:0006366), DNA-templated transcription, initiation (GO:0006352).		

Note: The Pearson correlation analysis is presented with and without the transcriptional values of the *ACT1* gene, as a way to assess the effect that this gene has in the stability of the data set.
[a]Data from Gasch et al.

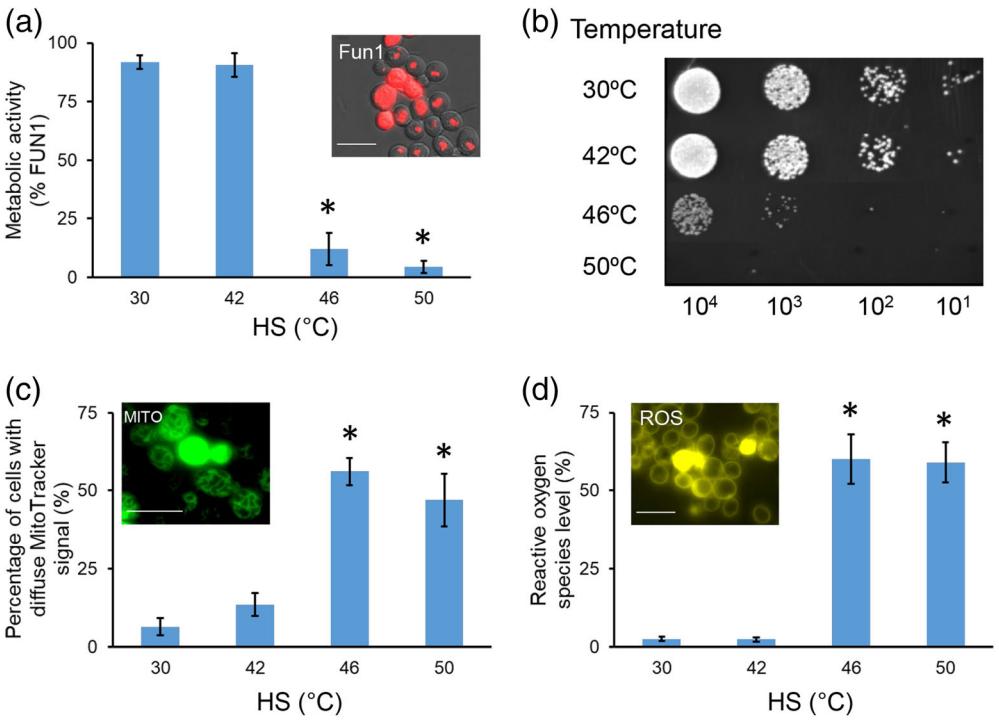

FIGURE 4 Evaluation of phenotypes under heat shock (HS) stress. (a) Percentage of metabolically active cells under different temperatures. Metabolic activity is determined by FUN1-positive cells, and representative image of FUN1 staining is shown. Metabolically active cells show concentrated red staining in the vacuole while nonactive cells give out a uniform red glow. (b) Spot tests of cells after the induction of HS stress to investigate cell survival; 0.2 OD_{600} of cells are diluted in 10-fold series and spotted on YPD plates. (c) Percentage of cells with damaged mitochondria under different temperatures. Mitochondria are stained with MitoTracker. Cells showing an intense and diffuse fluorescence are considered as mitochondrial damage. (d) Fractions of reactive oxygen species (ROS)-positive cells under different temperatures. Cells are stained with DHR123. Cells showing an intense fluorescence are considered as ROS positive. For these measurements, at least 300 cells were counted in each group. Results are shown as average values ± SD from three biological experiments. Asterisks (*) indicate significant differences compared with control strain at 30°C ($p < 0.05$). Scale = 10 μm [Colour figure can be viewed at wileyonlinelibrary.com]

transcription of *ERO1* and *KAR2* was measured as positive controls. *ERO1* (endoplasmic reticulum oxireductin 1) encodes thiol oxidase required for oxidative protein folding in the ER, which is essential for maintaining ER redox balance (GO:0006457). Whereas *KAR2* is an essential gene for cellular viability, it is involved in diverse cellular processes, such as protein folding (GO:0006457), transmembrane

transport (GO:0055085), cell wall organization or biogenesis (GO:0071554), carbohydrate metabolic process (GO:0005975), and proteolysis involved in cellular protein catabolic process (GO:0051603), and so forth (https://www.yeastgenome.org/goSlimMapper). The transcription of *ERO1* and *KAR2* was significantly increased at 42°C and 46°C, compared with control strain at 30°C ($p < 0.05$; Figure 5), indicating that the stress has been induced. The transcription levels of *ERO1* were 8.2- and 21.7-fold higher at 42°C and 46°C, respectively, compared with control strain at 30°C. And the transcription levels of *KAR2* were 12.1- and 6.3-fold higher at 42°C and 46°C, respectively, compared with control strain at 30°C.

The stress response genes (*UBI4* and *RRP5*) and reference genes (*MEX67* and *SSY1*) identified as markers of HS stress were evaluated (Figure 5). The transcription levels of *UBI4* were 17- and 23-fold higher at 42°C and 46°C, respectively, compared with control strain at 30°C ($p < 0.05$). The transcription levels of *RRP5* were ninefold and sixfold higher at 42°C and 46°C, respectively, compared with control strain at 30°C ($p < 0.05$). There were no significant changes for *MEX67* and *SSY1* transcriptional levels at 42°C and 46°C, compared with control strain at 30°C ($p > 0.05$; Figure 5).

3.7 | Assessment of HS stress response under DTT stress

To test if the transcriptional response is the HS-specific stress response, cells were challenged with different concentrations of DTT (2.5, 5.0, and 7.5 mM, respectively). The specific growth rate was first tested after DTT treatment. Comparing with the control strain without DTT treatment, the 2.5 mM of DTT treatment caused a 25% decrease in growth (from 0.48 to 0.36 h^{-1}, $p < 0.05$) and the 5.0 mM of DTT treatment further reduced the specific growth rate (from 0.48 to 0.10 h^{-1}, $p < 0.05$). The metabolic activity measurement showed that DTT treatment significantly reduced the percentage of cells with CIVS structures in a dosage-dependent way. The fractions of metabolically active cells were 93.3% in control strain without DTT treatment, comparing with 72.7%, 58.4%, and 3% with 2.5, 5.0, and 7.5 mM of DTT added, respectively ($p < 0.05$; Figure 6a). The DTT treatment also significantly increased mitochondrial damage and ROS production ($p < 0.05$; Figure 6b,c).

To test if the *UBI4* and *RRP5* are the HS-specific stress response genes, their transcription levels were further evaluated under DTT stress condition (Figure 7). The results showed that the transcription levels of *UBI4* were threefold and fivefold increase at 2.5- and 7.5-mM DTT treatment compared with control strain without DTT treatment, which were sixfold lower than its expression under the HS stress. The transcription levels of *RRP5* under DTT stress were also significantly lower than its expression under the HS stress ($p < 0.05$), which were 1.6- and 2.5-fold increase at 2.5- and 7.5-mM DTT treatment compared with control strain without DTT treatment. These transcriptional differences between HS stress and DTT stress were not observed in the transcription of *ERO1* and *KAR2*, which showed similar upregulated levels in both conditions (Figures 5 and 7). There were no significant changes for *MEX67* and *SSY1* transcriptional levels at different concentrations of DTT treatment compared with control strain without DTT treatment ($p > 0.05$; Figure 7). This result showed that our statistical data analysis can be used as a reliable tool to identify specifically stress-induced genes and that *UBI4* and *RRP5* genes can be used as HS-specific stress response genes. The uninduced and stable transcriptional expression of *MEX67* and *SSY1* in both HS stress and DTT stresses showed that the same approach can identify reference genes under different stress conditions.

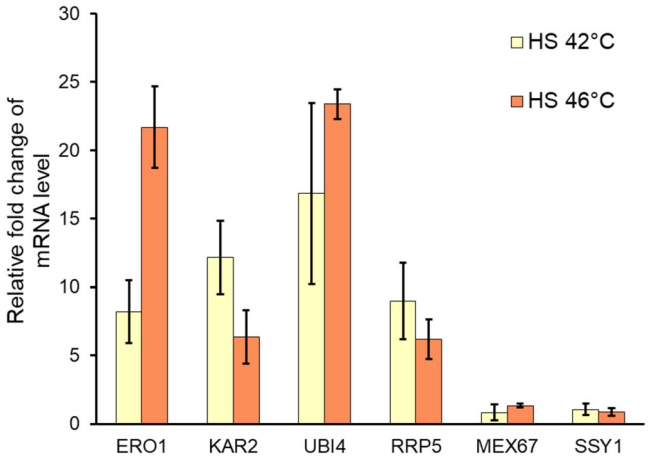

FIGURE 5 The transcriptional response of the heat shock (HS) stress. The test stress response genes for the HS stress are *UBI4* and *RRP5*. The test reference genes for the HS stress are *MEX67* and *SSY1*. The positive controls are *ERO1* and *KAR2* genes. Results from HS stress are normalized to the control strain growing at 30°C. The transcriptional values are shown as the average of three independent biological replicates ± SD [Colour figure can be viewed at wileyonlinelibrary.com]

4 | DISCUSSION

In this work, we developed a bioinformatics pipeline for selecting relevant genes that were then used for setting up a proof of concept for a simple and reliable assay that is to be used for assessing stress-specific gene transcription for cell stress and potentially cell fate prediction. The need for such assays comes from the fermentation industry where in some cases, the production losses go up to 50% (personal communication) due to cell damage and loss. The aim of such assays is to be used very early on before other standard industrial parameters show significant changes, in large scale and by nonspecialist staff who would in an ideal case be able to make quick decisions, early on, about changing fermentation parameters or terminating the process. This would lead to millions of saved USD in the production.

We selected genes that were specifically upregulated during different types of stress, which were not only specific for different types of stress but also displayed different transcriptional patterns during mild and lethal stresses. A search for stress response genes in a

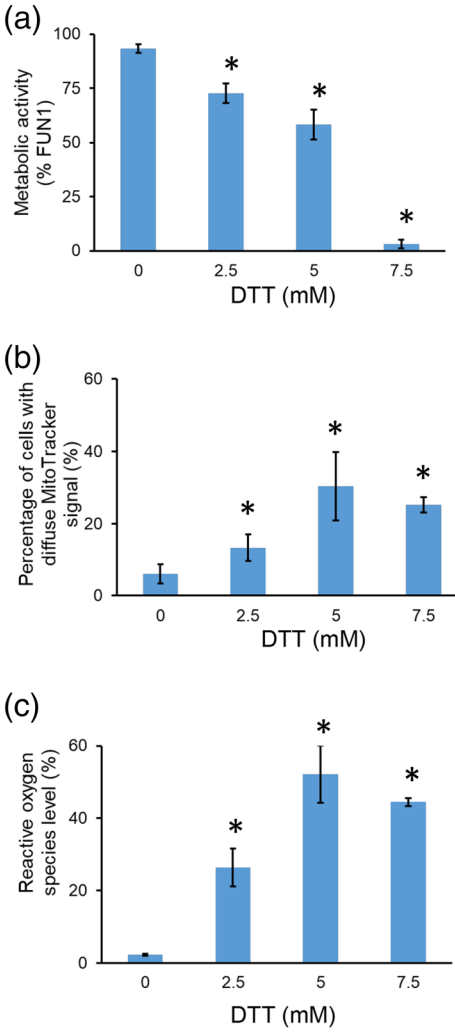

FIGURE 6 Evaluation of phenotypes under dithiothreitol (DTT) stress. (a) Percentage of metabolically active cells with different concentrations of DTT treatment. Metabolic activity is determined by FUN1-positive cells. (b) Percentage of cells with damaged mitochondria under different concentrations of DTT treatment. Mitochondria are stained with MitoTracker. (c) Fractions of reactive oxygen species (ROS)-positive cells with different concentrations of DTT treatment. Cells are stained with DHR123. For these measurements, at least 300 cells were counted in each group. Results are shown as average values ± SD from three biological experiments. Asterisks (*) indicate significant differences compared with control strain without DTT treatment ($p < 0.05$) [Colour figure can be viewed at wileyonlinelibrary.com]

genome wide transcription data set comprising 10 different stresses at different time points was performed, based on initial experimental data from Gasch et al. (2000). The correlation and PCA analyses were performed. This allowed for testing the feasibility of finding stress-specific response genes. Additionally, the confirmation qPCR tests, and the phenotypic characterizations, were conducted in the strain CEN.PK113-11C, which is very different from the DBY strain (Strucko et al., 2015), which was used to collect the initial data (Gasch et al., 2000), pointing out to the robustness of the identified targets across very diverse strains.

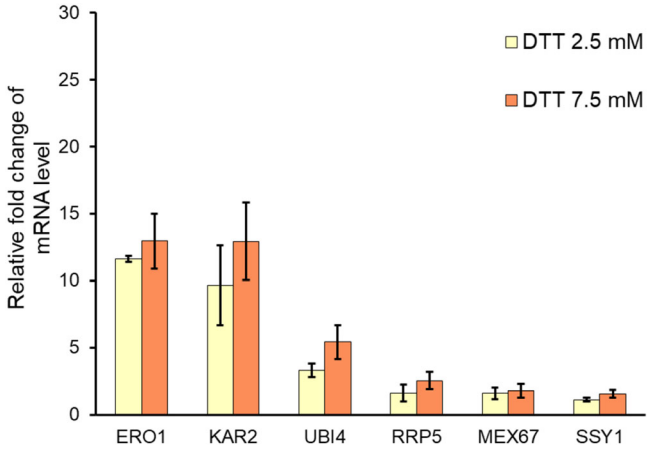

FIGURE 7 The transcriptional response of heat shock (HS) stress response genes and reference genes under dithiothreitol (DTT) stress. The test HS stress response genes are *UBI4* and *RRP5*. The test reference genes for the HS stress are *MEX67* and *SSY1*. The positive controls are *ERO1* and *KAR2* genes. Results from different concentrations of DTT treatment are normalized to the control strain without DTT treatment. The transcriptional values are shown as the average of three independent biological replicates ± SD [Colour figure can be viewed at wileyonlinelibrary.com]

After the statistical analyses, it was clear that stresses such as the HS, the stationary phase, and the nitrogen depletion are significantly different in their transcriptional responses (Figure 3). In the other stress conditions, the diamide, H_2O_2, AA starvation, hyperosmotic and hypoosmotic, DTT, and menadione, the overall transcriptional response was more similar (Figure 3). The HS and the DTT stresses were selected as examples for further experimental verification with a significant degree of correlation and covariance.

All living cells need to balance resources (i.e., energy and building blocks) between cell growth and division, and cell maintenance including stress responses. Activation of defense strategies is often coordinated with arrest of cell growth (Zakrzewska et al., 2011). Yeast cells are able to respond to HS stress with upregulation of hundreds of genes. A core set of upregulated genes are termed heat shock proteins (HSP), which prevent or reverse the protein aggregation under HS stress (Hartl et al., 2011). At 42°C, as expected, cells showed significantly decreased specific growth rate, whereas the metabolic activity (as assessed by CIVs formation) and viability were not affected, compared with the control at 30°C (Figure 4a,b). When the "buffering capacity" of the HS response (HSR) is inadequate to keep homeostasis, cell death will remove irreversibly damaged cells (Morano et al., 2012), which is confirmed in our experiments as we found significantly elevated fractions of dead cells and arrested cell growth at 46°C and 50°C (Figure 4a,b). A comprehensive omics study from different levels of HS stress showed that most of heat-induced genes are required to confer stress resistance and help to maintain proteostasis. At 37°C and 42°C, cells can be recovered after HSR, and the mRNA levels and protein turnover normalize again. At 46°C, HSR cannot balance impaired protein homeostasis; therefore, cell growth

stops (Mühlhofer et al., 2019). It is in accordance with our findings at 46°C and 50°C.

Studies have showed that the tolerance of HS is closely linked to aerobic metabolism and oxidative stress. Yeast cells cultured anaerobically are more resistant to HS than those grown aerobically (Davidson et al., 1996). Lacking antioxidant enzymes, for example, superoxide dismutase (SOD), can convert cells to hypersensitivity to HS stress (Davidson et al., 1996). Under aerobic condition, the main flux of oxygen goes through the electron transport chain located to the mitochondrial network. The mitochondria are a key organelle in the energy metabolism, stress response, and cell survival. This organelle is constituted of a dynamic and complex network of individual organelles, which interact and form dynamic networks. The dynamic of such network is maintained by the equilibrium between fusion–fission events, and its morphology is a hallmark to determine cellular stress (Youle & van der Bliek, 2012). Oxidative stress is often accompanied by impaired mitochondrial function and increased ROS production, which may exacerbate stress progression through oxidative damage to cellular structures, proteins, lipids, and DNA (Lin & Beal, 2006). Our study showed that under HS stress, mitochondrial network was damaged in more than 50% of cell population at 46°C and 50°C, comparing with 6% in control strain at 30°C (Figure 4c). It was accompanied by the significantly increased ROS-positive fractions ($p < 0.05$; Figure 4d).

In this study, we identified two HS response genes: *UBI4* and *RRP5*. Their transcript levels were significantly upregulated during the HS treatment (Figure 5), whereas the levels were much lower under the DTT stress (Figure 7). This indicates that our approach can identify genes to be used as specific stress response genes (in this case for the HS stress). In yeast, *UBI4* is one of the four ubiquitin genes, which contains five head-to-tail ubiquitin elements and encodes a polyubiquitin precursor protein (Ozkaynak et al., 1987). Ubiquitin homeostasis is critical for cell maintenance and growth (Chen & Petranovic, 2016). Study showed that *ubi4* mutants are hypersensitive to high temperatures and *UBI4* is required for chronic heat stress of sublethal high temperatures (Finley et al., 1987). This multiunit structure encoded by *UBI4* enables cells to quickly produce large amounts of ubiquitin needed to cope with sudden stress, and the repeat numbers of *UBI4* influence the protein homeostasis and cellular survival during heat stress (Gemayel et al., 2017). *RRP5* encodes a large, highly conserved ribosome synthesis protein, required for maturation of 18S and 5.8rRNAs (Lebaron et al., 2013; Venema & Tollervey, 1996). RRP5 can mediate the crosstalk between 40S and 60S assembly pathways to ensure balanced levels of the two subunits, which is important during early preribosome assembly (Khoshnevis et al., 2019). In the same manner, we can identify and propose new reference genes under these stress conditions. *MEX67* and *SSY1* showed stable low expression in both HS and DTT stresses (Figures 5 and S4).

In summary, we have developed a bioinformatics pipeline that can be used for at least two different industrial production yeast strains and that can provide a basis for development of assays based on qPCR tests of selected relevant genes and can provide cheap, simple, and quick assessment of the state, and potentially the fate, of the culture, which is then translated in significant reduction of costs due to suboptimal or failed fermentations. The proof-of-concept assay could be a useful tool for identifying stress response genes and reference genes under 10 different stress conditions, many of them of relevance in industrial processes.

ACKNOWLEDGEMENTS

This study was financially supported by the Kristina Stenborg Foundation (grant number: C2012/1241), the Chalmers Foundation (grant number: C2007/778), and the Novo Nordisk Foundation Center for Biosustainability (grant number: 21210022).

CONFLICT OF INTEREST

The authors declare no conflict of interest.

AUTHOR CONTRIBUTIONS

EM, XC, and DP designed the project. EM, AJMA, MJ, and XC carried out the experiments; EM carried out the transcriptional data analysis. All authors contributed to project development, interpretation of results, and writing and editing of the manuscript.

DATA AVAILABILITY STATEMENT

The data that support the findings of this study are available from the corresponding author upon reasonable request.

ORCID

Xin Chen https://orcid.org/0000-0003-2788-1314

REFERENCES

Aad, G., Abbott, B., Abdallah, J., Abdelalim, A. A., Abdesselam, A., Abdinov, O., … Zutshi, V. (2010). Search for new particles in two-jet final states in 7 TeV proton-proton collisions with the ATLAS detector at the LHC. *Physical Review Letters*, *105*(16), 161801. https://doi.org/10.1103/PhysRevLett.105.161801

Andréasson, C., Ott, M., & Büttner, S. (2019). Mitochondria orchestrate proteostatic and metabolic stress responses. *EMBO Reports*, *20*(10), e47865. https://doi.org/10.15252/embr.201947865

Becker, C., Hammerle-Fickinger, A., Riedmaier, I., & Pfaffl, M. W. (2010). mRNA and microRNA quality control for RT-qPCR analysis. *Methods*, *50*(4), 237–243. https://doi.org/10.1016/j.ymeth.2010.01.010

Botstein, D., Chervitz, S. A., & Cherry, J. M. (1997). Yeast as a model organism. *Science*, *277*(5330), 1259–1260. https://doi.org/10.1126/science.277.5330.1259

Botstein, D., & Fink, G. R. (1988). Yeast: An experimental organism for modern biology. *Science*, *240*(4858), 1439–1443. https://doi.org/10.1126/science.3287619

Botstein, D., & Fink, G. R. (2011). Yeast: An experimental organism for 21st Century biology. *Genetics*, *189*(3), 695–704. https://doi.org/10.1534/genetics.111.130765

Bustin, S. A., Benes, V., Garson, J. A., Hellemans, J., Huggett, J., Kubista, M., Mueller, R., Nolan, T., Pfaffl, M. W., Shipley, G. L., Vandesompele, J., & Wittwer, C. T. (2009). The MIQE guidelines: Minimum information for publication of quantitative real-time PCR experiments. *Clinical Chemistry*, *55*(4), 611–622. https://doi.org/10.1373/clinchem.2008.112797

Carmona-Gutierrez, D., Bauer, M. A., Zimmermann, A., Aguilera, A., Austriaco, N., Ayscough, K., … Madeo, F. (2018). Guidelines and

recommendations on yeast cell death nomenclature. *Microb Cell*, *5*(1), 4–31. https://doi.org/10.15698/mic2018.01.607

Carmona-Gutierrez, D., Eisenberg, T., Buttner, S., Meisinger, C., Kroemer, G., & Madeo, F. (2010). Apoptosis in yeast: Triggers, pathways, subroutines. *Cell Death and Differentiation*, *17*(5), 763–773. https://doi.org/10.1038/cdd.2009.219

Chen, X., Bisschops, M. M. M., Agarwal, N. R., Ji, B., Shanmugavel, K. P., & Petranovic, D. (2017). Interplay of energetics and ER stress exacerbates Alzheimer's amyloid-β (Aβ) toxicity in yeast. *Frontiers in Molecular Neuroscience*, *10*, 232–232. https://doi.org/10.3389/fnmol.2017.00232

Chen, X., & Petranovic, D. (2016). Role of frameshift ubiquitin B protein in Alzheimer's disease. *Wiley Interdisciplinary Reviews. Systems Biology and Medicine*, *8*(4), 300–313. https://doi.org/10.1002/wsbm.1340

Cherry, J. M., Ball, C., Weng, S., Juvik, G., Schmidt, R., Adler, C., Dunn, B., Dwight, S., Riles, L., Mortimer, R. K., & Botstein, D. (1997). Genetic and physical maps of *Saccharomyces cerevisiae*. *Nature*, *387*(6632 Suppl), 67–73. https://doi.org/10.1038/387s067

Cherry, J. M., Hong, E. L., Amundsen, C., Balakrishnan, R., Binkley, G., Chan, E. T., Christie, K. R., Costanzo, M. C., Dwight, S. S., Engel, S. R., Fisk, D. G., Hirschman, J. E., Hitz, B. C., Karra, K., Krieger, C. J., Miyasato, S. R., Nash, R. S., Park, J., Skrzypek, M. S., … Wong, E. D. (2012). Saccharomyces Genome Database: The genomics resource of budding yeast. *Nucleic Acids Research*, *40*(Database issue), D700–D705. https://doi.org/10.1093/nar/gkr1029

Davidson, J. F., Whyte, B., Bissinger, P. H., & Schiestl, R. H. (1996). Oxidative stress is involved in heat-induced cell death in *Saccharomyces cerevisiae*. *Proceedings of the National Academy of Sciences of the United States of America*, *93*(10), 5116–5121. https://doi.org/10.1073/pnas.93.10.5116

Development Core Team, R. (2011). R: A language and environment for statistical computing (Vol. *1*).

Entian, K.-D., & Kötter, P. (1998). 23 yeast mutant and plasmid collections. In A. J. P. Brown & M. Tuite (Eds.), *Methods in microbiology* (Vol. 26, pp. 431–449). Academic Press.

Fannjiang, Y., Cheng, W. C., Lee, S. J., Qi, B., Pevsner, J., McCaffery, J. M., … Hardwick, J. M. (2004). Mitochondrial fission proteins regulate programmed cell death in yeast. *Genes & Development*, *18*(22), 2785–2797. https://doi.org/10.1101/gad.1247904

Finley, D., Özkaynak, E., & Varshavsky, A. (1987). The yeast polyubiquitin gene is essential for resistance to high temperatures, starvation, and other stresses. *Cell*, *48*(6), 1035–1046. https://doi.org/10.1016/0092-8674(87)90711-2

Gasch, A. P. (2007). Comparative genomics of the environmental stress response in ascomycete fungi. *Yeast*, *24*(11), 961–976. https://doi.org/10.1002/yea.1512

Gasch, A. P., Spellman, P. T., Kao, C. M., Carmel-Harel, O., Eisen, M. B., Storz, G., Botstein, D., & Brown, P. O. (2000). Genomic expression programs in the response of yeast cells to environmental changes. *Molecular Biology of the Cell*, *11*(12), 4241–4257. https://doi.org/10.1091/mbc.11.12.4241

Gemayel, R., Yang, Y., Dzialo, M. C., Kominek, J., Vowinckel, J., Saels, V., van Huffel, L., van der Zande, E., Ralser, M., Steensels, J., Voordeckers, K., & Verstrepen, K. J. (2017). Variable repeats in the eukaryotic polyubiquitin gene ubi4 modulate proteostasis and stress survival. *Nature Communications*, *8*(1), 397–397. https://doi.org/10.1038/s41467-017-00533-4

Goffeau, A., Barrell, B. G., Bussey, H., Davis, R. W., Dujon, B., Feldmann, H., … Oliver, S. G. (1996). Life with 6000 genes. *Science*, *274*(5287), 546–567. https://doi.org/10.1126/science.274.5287.546

Hartl, F. U., Bracher, A., & Hayer-Hartl, M. (2011). Molecular chaperones in protein folding and proteostasis. *Nature*, *475*(7356), 324–332. https://doi.org/10.1038/nature10317

Hauptmann, P., & Lehle, L. (2008). Kex1 protease is involved in yeast cell death induced by defective N-glycosylation, acetic acid, and chronological aging. *The Journal of Biological Chemistry*, *283*(27), 19151–19163. https://doi.org/10.1074/jbc.M801303200

Herrero, E., Ros, J., Belli, G., & Cabiscol, E. (2008). Redox control and oxidative stress in yeast cells. *Biochimica et Biophysica Acta*, *1780*(11), 1217–1235. https://doi.org/10.1016/j.bbagen.2007.12.004

Jung, P. P., Christian, N., Kay, D. P., Skupin, A., & Linster, C. L. (2015). Protocols and programs for high-throughput growth and aging phenotyping in yeast. *PLoS ONE*, *10*(3), e0119807. https://doi.org/10.1371/journal.pone.0119807

Kachroo, A. H., Laurent, J. M., Yellman, C. M., Meyer, A. G., Wilke, C. O., & Marcotte, E. M. (2015). Evolution. Systematic humanization of yeast genes reveals conserved functions and genetic modularity. *Science*, *348*(6237), 921–925. https://doi.org/10.1126/science.aaa0769

Keij, J. F., Bell-Prince, C., & Steinkamp, J. A. (2000). Staining of mitochondrial membranes with 10-nonyl acridine orange MitoFluor Green, and MitoTracker Green is affected by mitochondrial membrane potential altering drugs. *Cytometry: The Journal of the International Society for Analytical Cytology*, *39*(3), 203–210. https://doi.org/10.1002/(SICI)1097-0320(20000301)39:3<203::AID-CYTO5>3.0.CO;2-Z

Khoshnevis, S., Liu, X., Dattolo, M. D., & Karbstein, K. (2019). Rrp5 establishes a checkpoint for 60S assembly during 40S maturation. *RNA*, *25*(9), 1164–1176. https://doi.org/10.1261/rna.071225.119

Kim, I. S., Sohn, H. Y., & Jin, I. (2011). Adaptive stress response to menadione-induced oxidative stress in *Saccharomyces cerevisiae* KNU5377. *Journal of Microbiology*, *49*(5), 816–823. https://doi.org/10.1007/s12275-011-1154-6

Kimata, Y., Ishiwata-Kimata, Y., Yamada, S., & Kohno, K. (2006). Yeast unfolded protein response pathway regulates expression of genes for anti-oxidative stress and for cell surface proteins. *Genes to Cells*, *11*(1), 59–69. https://doi.org/10.1111/j.1365-2443.2005.00921.x

Kohno, K., Normington, K., Sambrook, J., Gething, M. J., & Mori, K. (1993). The promoter region of the yeast KAR2 (BiP) gene contains a regulatory domain that responds to the presence of unfolded proteins in the endoplasmic reticulum. *Molecular and Cellular Biology*, *13*(2), 877–890. https://doi.org/10.1128/mcb.13.2.877

Kwolek-Mirek, M., & Zadrag-Tecza, R. (2014). Comparison of methods used for assessing the viability and vitality of yeast cells. *FEMS Yeast Research*, *14*(7), 1068–1079. https://doi.org/10.1111/1567-1364.12202

Lebaron, S., Segerstolpe, A., French, S. L., Dudnakova, T., de Lima Alves, F., Granneman, S., … Tollervey, D. (2013). Rrp5 binding at multiple sites coordinates pre-rRNA processing and assembly. *Molecular Cell*, *52*(5), 707–719. https://doi.org/10.1016/j.molcel.2013.10.017

Lin, M. T., & Beal, M. F. (2006). Mitochondrial dysfunction and oxidative stress in neurodegenerative diseases. *Nature*, *443*(7113), 787–795. https://doi.org/10.1038/nature05292

Livnat-Levanon, N., Kevei, E., Kleifeld, O., Krutauz, D., Segref, A., Rinaldi, T., Erpapazoglou, Z., Cohen, M., Reis, N., Hoppe, T., & Glickman, M. H. (2014). Reversible 26S proteasome disassembly upon mitochondrial stress. *Cell Reports*, *7*(5), 1371–1380. https://doi.org/10.1016/j.celrep.2014.04.030

Longo, V. D., Ellerby, L. M., Bredesen, D. E., Valentine, J. S., & Gralla, E. B. (1997). Human Bcl-2 reverses survival defects in yeast lacking superoxide dismutase and delays death of wild-type yeast. *The Journal of Cell Biology*, *137*(7), 1581–1588. https://doi.org/10.1083/jcb.137.7.1581

Madeo, F., Fröhlich, E., & Fröhlich, K. U. (1997). A yeast mutant showing diagnostic markers of early and late apoptosis. *The Journal of Cell Biology*, *139*(3), 729–734. https://doi.org/10.1083/jcb.139.3.729

Madeo, F., Herker, E., Maldener, C., Wissing, S., Lachelt, S., Herlan, M., … Frohlich, K. U. (2002). A caspase-related protease regulates apoptosis

in yeast. *Molecular Cell*, *9*(4), 911–917. https://doi.org/10.1016/S1097-2765(02)00501-4

Mansson, R., Tsapogas, P., Akerlund, M., Lagergren, A., Gisler, R., & Sigvardsson, M. (2004). Pearson correlation analysis of microarray data allows for the identification of genetic targets for early B-cell factor. *The Journal of Biological Chemistry*, *279*(17), 17905–17913. https://doi.org/10.1074/jbc.M400589200

Martelli, A. M., Zweyer, M., Ochs, R. L., Tazzari, P. L., Tabellini, G., Narducci, P., & Bortul, R. (2001). Nuclear apoptotic changes: An overview. *Journal of Cellular Biochemistry*, *82*(4), 634–646. https://doi.org/10.1002/jcb.1186

Mirisola, M. G., Braun, R. J., & Petranovic, D. (2014). Approaches to study yeast cell aging and death. *FEMS Yeast Research*, *14*(1), 109–118. https://doi.org/10.1111/1567-1364.12112

Morano, K. A., Grant, C. M., & Moye-Rowley, W. S. (2012). The response to heat shock and oxidative stress in *Saccharomyces cerevisiae*. *Genetics*, *190*(4), 1157–1195. https://doi.org/10.1534/genetics.111.128033

Mühlhofer, M., Berchtold, E., Stratil, C. G., Csaba, G., Kunold, E., Bach, N. C., Sieber, S. A., Haslbeck, M., Zimmer, R., & Buchner, J. (2019). The heat shock response in yeast maintains protein homeostasis by chaperoning and replenishing proteins. *Cell Reports*, *29*(13), 4593–4607.e4598. https://doi.org/10.1016/j.celrep.2019.11.109

Munoz, A. J., Wanichthanarak, K., Meza, E., & Petranovic, D. (2012). Systems biology of yeast cell death. *FEMS Yeast Research*, *12*(2), 249–265. https://doi.org/10.1111/j.1567-1364.2011.00781.x

Munoz-Arellano, A. J., Chen, X., Molt, A., Meza, E., & Petranovic, D. (2018). Different expression levels of human mutant ubiquitin B^{+1} (UBB^{+1}) can modify chronological lifespan or stress resistance of *Saccharomyces cerevisiae*. *Frontiers in Molecular Neuroscience*, *11*, 200. https://doi.org/10.3389/fnmol.2018.00200

Nolan, J., de Hoon, M. J. L., Imoto, S., & Miyano, S. (2004). Open source clustering software. *Bioinformatics*, *20*(9), 1453–1454. https://doi.org/10.1093/bioinformatics/bth078

Nolan, T., Hands, R. E., & Bustin, S. A. (2006). Quantification of mRNA using real-time RT-PCR. *Nature Protocols*, *1*(3), 1559–1582. https://doi.org/10.1038/nprot.2006.236

Ouyang, M., Welsh, W. J., & Georgopoulos, P. (2004). Gaussian mixture clustering and imputation of microarray data. *Bioinformatics*, *20*(6), 917–923. https://doi.org/10.1093/bioinformatics/bth007

Ozkaynak, E., Finley, D., Solomon, M. J., & Varshavsky, A. (1987). The yeast ubiquitin genes: A family of natural gene fusions. *The EMBO Journal*, *6*(5), 1429–1439. https://doi.org/10.1002/j.1460-2075.1987.tb02384.x

Petranovic, D., & Nielsen, J. (2008). Can yeast systems biology contribute to the understanding of human disease? *Trends in Biotechnology*, *26*(11), 584–590. https://doi.org/10.1016/j.tibtech.2008.07.008

Petranovic, D., Tyo, K., Vemuri, G. N., & Nielsen, J. (2010). Prospects of yeast systems biology for human health: Integrating lipid, protein and energy metabolism. *FEMS Yeast Research*, *10*(8), 1046–1059. https://doi.org/10.1111/j.1567-1364.2010.00689.x

Qin, Y., Lu, M., & Gong, X. (2008). Dihydrorhodamine 123 is superior to 2,7-dichlorodihydrofluorescein diacetate and dihydrorhodamine 6G in detecting intracellular hydrogen peroxide in tumor cells. *Cell Biology International*, *32*(2), 224–228. https://doi.org/10.1016/j.cellbi.2007.08.028

Reich, J. G., & Meiske, W. (1985). Adaptation games between microorganisms sharing a common substrate niche. *Journal of Basic Microbiology*, *25*(8), 513–519. https://doi.org/10.1002/jobm.3620250813

Rozen, S., & Skaletsky, H. (2000). Primer3 on the WWW for general users and for biologist programmers. *Methods in Molecular Biology*, *132*, 365–386. https://doi.org/10.1385/1-59259-192-2:365

Ruijter, J. M., Ramakers, C., Hoogaars, W. M., Karlen, Y., Bakker, O., van den Hoff, M. J., & Moorman, A. F. (2009). Amplification efficiency: Linking baseline and bias in the analysis of quantitative PCR data. *Nucleic Acids Research*, *37*(6), e45. https://doi.org/10.1093/nar/gkp045

Sanchez, Y., & Lindquist, S. L. (1990). HSP104 required for induced thermotolerance. *Science*, *248*(4959), 1112–1115. https://doi.org/10.1126/science.2188365

Schefe, J. H., Lehmann, K. E., Buschmann, I. R., Unger, T., & Funke-Kaiser, H. (2006). Quantitative real-time RT-PCR data analysis: Current concepts and the novel "gene expression's CT difference" formula. *Journal of Molecular Medicine (Berlin, Germany)*, *84*(11), 901–910. https://doi.org/10.1007/s00109-006-0097-6

Strucko, T., Magdenoska, O., & Mortensen, U. H. (2015). Benchmarking two commonly used *Saccharomyces cerevisiae* strains for heterologous vanillin-β-glucoside production. *Metabolic Engineering Communications*, *2*, 99–108. https://doi.org/10.1016/j.meteno.2015.09.001

Szegezdi, E., Logue, S. E., Gorman, A. M., & Samali, A. (2006). Mediators of endoplasmic reticulum stress-induced apoptosis. *EMBO Reports*, *7*(9), 880–885. https://doi.org/10.1038/sj.embor.7400779

Teste, M. A., Duquenne, M., Francois, J. M., & Parrou, J. L. (2009). Validation of reference genes for quantitative expression analysis by real-time RT-PCR in *Saccharomyces cerevisiae*. *BMC Molecular Biology*, *10*, 99. https://doi.org/10.1186/1471-2199-10-99

Udvardi, M. K., Czechowski, T., & Scheible, W.-R. (2008). Eleven golden rules of quantitative RT-PCR. *20*(7), 1736–1737. https://doi.org/10.1105/tpc.108.061143

Uren, A. G., O'Rourke, K., Aravind, L. A., Pisabarro, M. T., Seshagiri, S., Koonin, E. V., & Dixit, V. M. (2000). Identification of paracaspases and metacaspases: Two ancient families of caspase-like proteins, one of which plays a key role in MALT lymphoma. *Molecular Cell*, *6*(4), 961–967. https://doi.org/10.1016/s1097-2765(00)00094-0

Vandesompele, J., De Preter, K., Pattyn, F., Poppe, B., Van Roy, N., De Paepe, A., & Speleman, F. (2002). Accurate normalization of real-time quantitative RT-PCR data by geometric averaging of multiple internal control genes. *Genome Biology*, *3*(7), Research0034. https://doi.org/10.1186/gb-2002-3-7-research0034

Venema, J., & Tollervey, D. (1996). RRP5 is required for formation of both 18S and 5.8S rRNA in yeast. *The EMBO Journal*, *15*(20), 5701–5714. https://doi.org/10.1002/j.1460-2075.1996.tb00954.x

Verghese, J., Abrams, J., Wang, Y., & Morano, K. A. (2012). Biology of the heat shock response and protein chaperones: Budding yeast (Saccharomyces cerevisiae) as a model system. *Microbiology and Molecular Biology Reviews*, *76*(2), 115–158. https://doi.org/10.1128/mmbr.05018-11

Weiner, J. (2013). pca3D: Three dimensional PCA plots.

Wloch-Salamon, D. M., & Bem, A. E. (2013). Types of cell death and methods of their detection in yeast *Saccharomyces cerevisiae*. *Journal of Applied Microbiology*, *114*(2), 287–298. https://doi.org/10.1111/jam.12024

Yang, H., Ren, Q., & Zhang, Z. (2008). Cleavage of Mcd1 by caspase-like protease Esp1 promotes apoptosis in budding yeast. *Molecular Biology of the Cell*, *19*(5), 2127–2134. https://doi.org/10.1091/mbc.e07-11-1113

Yeung, K. Y., & Ruzzo, W. L. (2001). Principal component analysis for clustering gene expression data. *Bioinformatics*, *17*(9), 763–774. https://doi.org/10.1093/bioinformatics/17.9.763

Youle, R. J., & van der Bliek, A. M. (2012). Mitochondrial fission, fusion, and stress. *Science*, *337*(6098), 1062–1065. https://doi.org/10.1126/science.1219855

Zakrzewska, A., van Eikenhorst, G., Burggraaff, J. E., Vis, D. J., Hoefsloot, H., Delneri, D., … Smits, G. J. (2011). Genome-wide analysis

of yeast stress survival and tolerance acquisition to analyze the central trade-off between growth rate and cellular robustness. *Molecular Biology of the Cell*, *22*(22), 4435–4446. https://doi.org/10.1091/mbc.e10-08-0721

SUPPORTING INFORMATION

Additional supporting information may be found online in the Supporting Information section at the end of this article.

How to cite this article: Meza, E., Muñoz-Arellano, A. J., Johansson, M., Chen, X., & Petranovic, D. (2021). Development of a method for heat shock stress assessment in yeast based on transcription of specific genes. *Yeast*, 1–17. https://doi.org/10.1002/yea.3658